# Bioconvective Ag-$Tio_2/H_2o$ Hybrid Nanofluid Flow Under the Influence of Brownian Motion and Thermophoresis

**Afsar Hossain Sarkar,**
Assistant Teacher, Department of Mathematics, Sahoorgachhi BMNH High School, Chanchal, Malda – 732123, West Bengal, India
E-mail: afsarhsarkar1986@gmail.com

**Dr. Annapurna Ramakrishna Sinde,**
Department of Mathematics, Dr. A P J Abdul Kalam University, Indore, Madhya Pradesh - 452016
E-mail: jayabhandari15@gmail.com

**Dr. Md Tausif Sk,**
Department of Mathematics, Acharya B N Seal College, Cooch Behar – 736101, West Bengal, India
Email: tausifdropbox@gmail.com

***Article Info***
***Page Number: 13293 – 13298***
***Publication Issue:***
***Vol 71 No. 4 (2022)***

**Abstract:** The aim of this study is to inspect the joined effects of attractive field and mixture nanofluid on bioconvection of a Casson nanofluid stream along a growing sheet coincided with gyrotactic microorganisms. The key fractional differential conditions are decreased to a bunch of nonlinear conventional differential conditions taking an aide of some suitable similitude changes. The mathematical aftermaths are determined by considering the bvp4c capability of Matlab. The effects of attractive field boundary, Brownian movement and attractive field on non-layered speed, nanoparticle fixation, temperature and thickness of self-moving microorganisms are deciphered through diagrams and outlines. The liquid speed close to the surface and the Nusselt number is reduce with attractive field. Attractive boundary upgrades oneself moving microorganism transition however a converse outcome is seen for thermophoresis. Likewise, the difference between the current outcomes with previously visited results is as one.

***Article History***
***Article Received:*** *25 October 2022*
***Revised:*** *30 November 2022*
***Accepted:*** *15 December 2022*

**Keywords:** MHD boundary layer flow; Bioconvection; gyrotactic microorganism; Casson Flow; Brownian Motion; Thermophoresis; Hybrid nanofluid.

## LITERATURE REVIEW:

The microorganisms are delegated "outrageous psychrophiles" (cold cherishing <0 ○C), "thermophiles" (between 50 ○C to 80 ○C), "hyperthermophiles" (between 80 ○C to 121 ○C) in light of the scope of temperature they can endure. The class of microorgan-isms is picked according to the prerequisite of the climate. Platt's report [1] was quick to examine the term bioconvection when he noticed the "Benard cells" structure because of the development polyg-onal examples of Tetrahymena (e.g., ciliate, lash) in thick cul-tures. The investigation of Ghorai and Slope [2] depicted the example arrangement in the microbial suspension through bioconvection.

Choi and Eastman [3] acquainted nanofluids with satisfy the requests of the business to have a liquid that has better intensity move qualities. These nanofluids are framed by suspend-ing the nanosized metal particles into the customary liquid. Xuan and associates [4,5] had caused the warm scattering in the movement to expand the course of intensity transport. These examinations demonstrated that the nanofluids track down various applications in the field of industrialized cooling, assembling of cleanser, biomedical applications, atomic reactors, central processor innovation, and so forth. Sinha and Misra [6] examined the prompted attractive field on magnetohydrody-namic (MHD) stream and it was reached

out to Bionanofluids by Basir et al. [7]. A portion of the purposes of magnetonanofluids are in MHD siphons and gas pedals, growth treatment, treatment of hyperther-mia, attractive reverberation imaging, sanitized gadgets, blockage evacuation in veins, MHD Power generators, and so forth, Refs. [8-13].
Nanofluids have significant power in microfluidic gadgets where lacking blending was constantly an issue. Moreover, the joule warming produced by dynamic blenders would have harmed the bio-applications. To defeat this issue, Kuznetsov [14] supplanted the dynamic blenders by motile microorganisms for upgrading the blending that lead to bioconvection in nanofluids. These microorganisms settle the nanoparticles suspended in the liquid and their development causes bio-convection. It is a phe-nomenon instigated by the aggregate development of self-pushed microorganisms. Kuznetsov broadened his review from bioconvec-tion to thermo bioconvection [15-17]. Aziz et al. [18] concentrated on the progression of nanofluids within the sight of gyrotactic microorganisms. Tham et al. [19,20] pushed on the significance of Bio-Convection in biomicrosystems for microfluidic types of gear. Shaw et al. [21] saw that the intensity move of a nanofluid was exceptionally influ-enced by Thermophoresis and Brownian movement. The examinations connected with bioconvective progression of nanofluid in permeable square depression within the sight of oxytactic microorganisms should be visible in [22] and [23]. Khan and Makinde [24,25] talked about bioconvection and noticed an expansion in the thickness of the base liquid because of the presence of microorganisms. Gireesha et al. [26,27] talked about the effect of Brownian movement and Thermophoresis on the three-layered bioconvective stream. These works spurred the designers to utilize bioconvection in biomicrosystems, biomedical, and microfluidic gadgets, power modules, wastewater treat-ments, assembling of liquor, pastry shop items, and so on.
Suspensions containing the single class nanoparticle may not have every one of the necessary qualities for a particular application. For instance, Al2O3 shows apparent synthetic inactivity and strength however will offer low warm conductivity. While, particles like aluminum (Al), silver (Ag), copper (Cu), and so on, have higher warm conductivity and are unsound and synthetically receptive. Thus, the blending of these nanoparticles with various physical and compound bonds structures nanofluid called mixture nanofluids and track down applications in atomic wellbeing, drug industry, cooling of electronic radiators, and so forth. Hayat and Nadeem [28] investigated that the hybridization of the liquid expanded the pace of intensity move. Chamkha and collaborators [29-31] examined the normal convection in the mixture nanofluid under attractive field in a square nook. Manjunatha et al. [32] talked about the progression of Cu Al2O3 H2O half breed nanofluid affected by factor thickness.
Ag TiO2 is a photocatalyst utilized as an antibacterial specialist since Ag improves the photocatalytic movement of TiO2 under the UV radiations by decreasing the recombination pace of photoexcited charge transporters that upgrades the natural builds as a result of the hydroxyl extremists framed by the protons [33-34]. The antibacterial action of Ag TiO2 against E-Coli under apparent light was read up for 0.15% silver doped titanium di-oxide with 0.05% centralization of dopant showed the most noteworthy decay pace of Rhodamine [35]. Moreover, the plasmonic design of Ag TiO2 incorporated with optical fiber can be utilized as dampness sensor. The axisymmetric stream of nanofluid assumes a significant part in medication and modern mechanical cycles and one of such is the stream past a slim needle. For example, in the clinical field, the majority of the created and delivered immunizations for human and creature security against sicknesses are comprised of lessened organisms in the liquid antibodies. These microbiomes of people and different creatures experience stream in numerous locales of the body, including the digestive system, stomach, urinary parcel, mouth, and lungs under different temperatures. In persistent blended tank bioreactors and photobioreactors, microorganisms are presented to laminar and tempestuous streams produced to upgrade their development and bioprocesses (like maturation) by guaranteeing supplement blending, gas trade, and ideal light openness. Subsequently, a genuine endeavor is had to dissect the effect homogenous/heterogeneous compound response on laminar progression of Ag TiO2 H2O crossover nanofluid through slender needle. The uniqueness of the issue is utilization of bioactive blenders to agglomeration of Ag TiO2 nanoparticles and avoids the statement of nanoparticles.

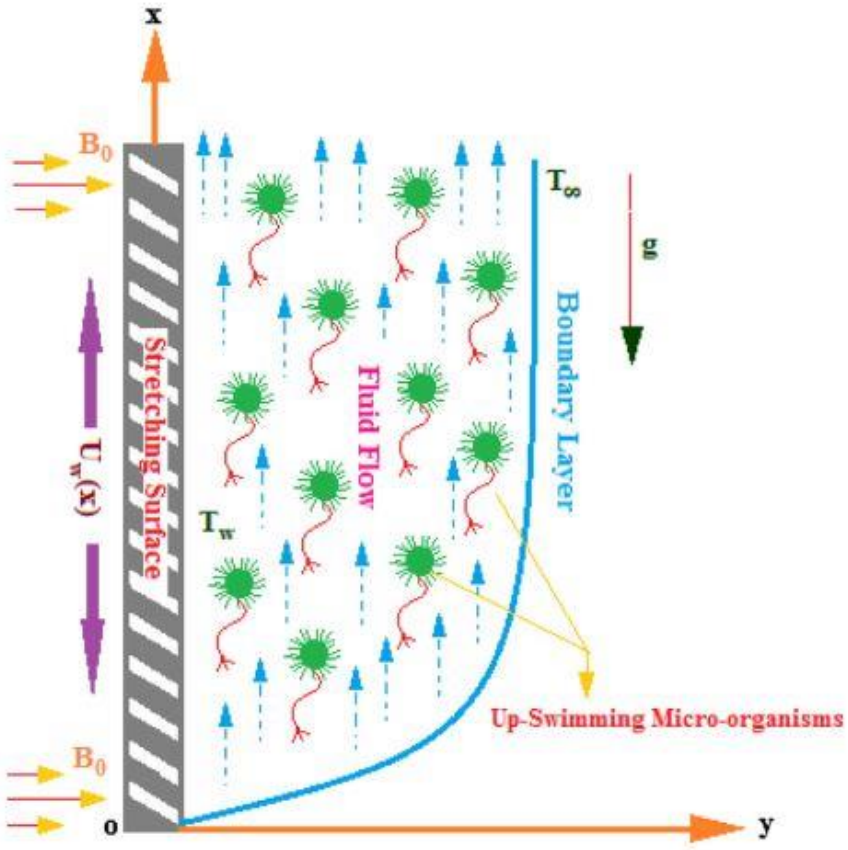


**Figure 1 Physical model of the flow**

**MATHEMATICAL FORMULATIONS:**

Here, we consider a nanofluid where the essential fluid is water, including electrically directing nano strong particles and gyrotactic microorganisms. We guess that the suspension of nano strong particles to be static and doesn't will generally combination inside liquid medium. It is likewise accepted that the presence of nanoparticles has no impact on the swimming course as well as on the speed of swim of microorganisms. This theory is solid just when nanoparticles fixation is lesser than 1%. In this way, for bioconvection strength, it is expected that the suspensions of nano strong particles are weakened in the fluid medium.

**Table 1: Properties of Nanofluid and Hybrid nanofluid:**

| Properties | Nanofluid | Hybrid nanofluid |
|---|---|---|
| Density $\left(kg.m^{-3}\right)$ | $\rho_{nf}=\left(1-\varphi\right)\rho_{bf}+\varphi\rho_{np}$ | $\rho_{hnf}=\left(1-\varphi_2\right)\begin{pmatrix}\left(1-\varphi_1\right)\rho_{bf}\\+\varphi_1\rho_{np1}\end{pmatrix}+\varphi_2\rho_{np2}$ |
| Heat capacity $\left(J.kg^{-1}.\mathrm{K}^{-1}\right)$ | $\left(\rho c_p\right)_{nf}=\left(1-\varphi\right)\left(\rho c_p\right)_{bf}+\varphi\left(\rho c_p\right)_{np}$ | $\left(\rho c_p\right)_{hnf}=\left(1-\varphi_2\right)\begin{pmatrix}\left(1-\varphi_1\right)\left(\rho c_p\right)_{bf}\\+\varphi_1\left(\rho c_p\right)_{np1}\end{pmatrix}+\varphi_2\left(\rho c_p\right)_{np2}$ |
| Viscosity $\left(\mathrm{N.m}^{-2}\right)$ | $\mu_{nf}=\frac{\mu_{bf}}{\left(1-\varphi\right)^{2.5}}$ | $\mu_{hnf}=\frac{\mu_{bf}}{\left(1-\varphi_1\right)^{2.5}\left(1-\varphi_2\right)^{2.5}}$ |

| | | |
|---|---|---|
| Thermal conductivity $\left(\mathrm{W.m^{-1}}.K^{-1}\right)$ | $\frac{\kappa_{nf}}{\kappa_{bf}}=\frac{\kappa_{np}+2\kappa_{bf}-2\varphi\left(\kappa_{bf}-\kappa_{np}\right)}{\kappa_{np}+2\kappa_{bf}+\varphi\left(\kappa_{bf}-\kappa_{np}\right)}$ | $\frac{\kappa_{hnf}}{\kappa_{nf}}=\frac{\kappa_{np2}+2\kappa_{nf}-2\varphi_2\left(\kappa_{nf}-\kappa_{np2}\right)}{\kappa_{np2}+2\kappa_{nf}+\varphi_2\left(\kappa_{nf}-\kappa_{np2}\right)}$, $\frac{\kappa_{nf}}{\kappa_{bf}}=\frac{\kappa_{np1}+2\kappa_{bf}-2\varphi_1\left(\kappa_{bf}-\kappa_{np1}\right)}{\kappa_{np1}+2\kappa_{bf}+\varphi_1\left(\kappa_{bf}-\kappa_{np1}\right)}$ |
| Electrical conductivity $\left(\mathrm{S.m^{-1}}\right)$ | $\frac{\sigma_{nf}}{\sigma_{bf}}=\frac{\sigma_{np}+2\sigma_{bf}-2\varphi\left(\sigma_{bf}-\sigma_{np}\right)}{\sigma_{np}+2\sigma_{bf}+\varphi\left(\sigma_{bf}-\sigma_{np}\right)}$ | $\frac{\sigma_{hnf}}{\sigma_{nf}}=\frac{\sigma_{np2}+2\sigma_{bf}-2\varphi_2\left(\sigma_{bf}-\sigma_{np2}\right)}{\sigma_{np2}+2\sigma_{bf}+\varphi_2\left(\sigma_{bf}-\sigma_{np2}\right)}$, $\frac{\sigma_{nf}}{\sigma_{bf}}=\frac{\sigma_{np1}+2\sigma_{bf}-2\varphi_1\left(\sigma_{bf}-\sigma_{np1}\right)}{\sigma_{np1}+2\sigma_{bf}+\varphi_1\left(\sigma_{bf}-\sigma_{np1}\right)}$ |

A direction is outlined having the beginning stage at the base corner of this sheet, where the x - hub stays upstanding and the y - hub stands opposite to the vertical. The movement of nanofluid stretches out to y > 0. Two comparable powers are applied to x - hub, however from inverse bearings to such an extent that the sheet is extended keeping up with the beginning fixed as displayed in Figure 1. The extended plate shifts along its surface with the extending speed uw=ax with "a" as a positive steady. A sidelong attractive motion with uniform strength B0 is executed oppositely to the plate. It is to be respected that there is no predominance of apparently carried out electric field. Attractive Reynolds number is immaterial; consequently, the inward attractive motion is negligible contrasted with apparently executed attractive transition.

In this audit, this temperature qualification is believed to be irrelevant. It is normal that the gathering of suspended nanoparticles is debilitate for the balance of the bioconvection instability. The nanoparticles are suspended using surfactants, with the objective that it prevents the agglomeration and surface strain among water and nanoparticles. Water, an optically thick medium is chosen to be the base fluid as it gives an environment that is the most suitable for the reliably passed gyrotactic microorganisms on to make due. This study expects round shape for the suspended nanoparticles.

The agglomeration of nanoparticles can be thwarted by using dynamic blenders either as engineered compounds or as microorganisms. Including dynamic blenders as manufactured compounds is neither effective nor holds the machine back from being hurt. In this manner, the use of self-prompted microorganisms is loved over manufactured substances. These microorganisms are heavier than the enveloping medium where they move and they are tending to swim upwards. These microorganisms answer explicit lifts by swimming in a specific heading [36]. Considering this response, the microorganisms are appointed gravitaxis, phototaxis, magnetotaxis, chemotaxis, gyrotaxis, etc, and the development of these microorganisms is obliged by gravity, light, appealing field, substance species, and mass point, independently. This study consolidates gyrotactic microorganisms that move due to the greatness of mass tendency and requires no additional power for its development. In this manner, including these microorganisms as powerful blenders is reasonable and useful. The microorganism's development in the nanofluid can be approximated as

$$m = M\,\mu + M\,\mu' - D_M \nabla M \tag{01}$$

Where $\mu' = \left(\frac{bW_c}{\Delta C}\right)\nabla C$. Here, both $\nabla C$ and changes in the centralization of the mass liquid $\Delta C$, are viewed as in the model because of the reality these microorganisms move in the homogeneous mass liquid during bioconvection.

A magnetic field $B_0$ is applied opposite to the progression of the electrically leading crossover nanofluid. The connection of attractive field with the actuated current J and the Lorentz force f is characterized as

$$f = J \times B = \sigma_{hnf} B_0^2 \left(v_x - U_{in}\right) \tag{02}$$

**Table 2: Thermophysical properties of base fluid and nanoparticles [33]:**

| | $\rho\left(kg.m^{-3}\right)$ | $\sigma\left(S.m^{-1}\right)$ | $\kappa\left(W.m^{-1}.K^{-1}\right)$ | $c_p\left(\mathrm{J.kg^{-1}}.K^{-1}\right)$ |
|---|---|---|---|---|
| $H_2O$ | 997.1 | $5.5\times10^{-6}$ | 0.6071 | 4179 |
| $Ag$ | 10490 | $63\times10^{6}$ | 429 | 235 |
| $TiO_2$ | 4250 | $2.4\times10^{6}$ | 8.953 | 686.2 |

The thermophysical properties are characterized in (Table 1) and their actual constants are yielded (Table 2). Under the above stated considerations, the fundamental equations can be gained from model projected by Xu and Pop [20] as follows:

$$\left.\begin{aligned}
&\frac{\partial u_x}{\partial x}+\frac{\partial u_y}{\partial y}=0\\
&u_x\frac{\partial u_x}{\partial x}+u_y\frac{\partial u_x}{\partial y}=\nu_{hnf}\frac{\partial^2 u_x}{\partial y^2}-\frac{\sigma_{hnf}B_0^2}{\rho_{hnf}}\left(u_x-U_{in}\right)\\
&u_x\frac{\partial T}{\partial x}+u_y\frac{\partial T}{\partial y}=\frac{\kappa_{hnf}}{\left(\rho c_p\right)_{hnf}}\frac{\partial^2 T}{\partial y^2}+\tau\left\{D_{BM}\frac{\partial C}{\partial y}\frac{\partial T}{\partial y}+\frac{D_{TP}}{T_{in}}\left(\frac{\partial T}{\partial y}\right)^2\right\}+\frac{1}{\left(\rho c_p\right)_{hnf}}\frac{\partial q_r}{\partial y}\\
&u_x\frac{\partial N}{\partial x}+u_y\frac{\partial N}{\partial y}=D_{BM}\frac{\partial^2 N}{\partial y^2}+\frac{D_{TP}}{T_{in}}\frac{\partial^2 T}{\partial y^2}\\
&u_x\frac{\partial M}{\partial x}+u_y\frac{\partial M}{\partial y}=D_{MO}\frac{\partial^2 M}{\partial y^2}-\left(\frac{bW_c}{\Delta C}\right)\frac{\partial}{\partial y}\left(M\frac{\partial N}{\partial y}\right)
\end{aligned}\right\} \tag{02}$$

With the appropriate boundary conditions are

$$\left.\begin{aligned}
&u_x=ax,u_y=0,T=T_w,D_{BM}\frac{\partial N}{\partial y}+\frac{D_{TP}}{T_{in}}\frac{\partial T}{\partial y}=0,M=M_w\ at\ y=0\\
&u_x\to U_{in},T\to T_{in},N\to N_{in},M\to M_{in}\ as\ y\to\infty
\end{aligned}\right\} \tag{03}$$

The energy equation in (02) is outlined utilizing the possibility of Rosseland [37] where warm radiation is accounted. The Plank number and the optical thickness are the significant boundaries worried about the impacts of radiation on the stream and intensity move. Obviously, during the disentanglement of Rosseland estimate, these two boundaries vanish after the determination. This determination will lead to another boundary called radiation boundary as the thorough radiation coefficient. This boundary is result of Board number and the optical thickness [38] and it is characterized as follows:

$$q_r=-\frac{4\sigma^*}{3k}\frac{\partial T^4}{\partial y} \tag{04}$$

This guess incorporates dissemination term that was presented in light of the hypothesis of preservation of energy. Since the temperature distinctions between $T_w$ and $T_\infty$ is thought to be essentially little, the Rosseland guess can be linearized by growing $T^4$ as per the Taylor series about $T_{in}$. The decreased development subsequent to dismissing the higher request terms is

$$T^4=4T_{in}^3T-3T_{in}^4 \tag{05}$$

By using this expression, the energy Eq. in (02) reduces to

$$u_x\frac{\partial T}{\partial x}+u_y\frac{\partial T}{\partial y}=\frac{\kappa_{hnf}}{\left(\rho c_p\right)_{hnf}}\frac{\partial^2 T}{\partial y^2}+\tau\left\{D_{BM}\frac{\partial C}{\partial y}\frac{\partial T}{\partial y}+\frac{D_{TP}}{T_{in}}\left(\frac{\partial T}{\partial y}\right)^2\right\}+\frac{16\sigma^* T_{in}^3}{3k\left(\rho c_p\right)_{hnf}}\frac{\partial^2 T}{\partial y^2} \tag{06}$$

The following similarity transformation transforms the partial differential equations to ordinary differential equations:

$$\left.\begin{aligned}&\xi=y\sqrt{\frac{a}{\nu_{bf}}},\omega(x,y)=\sqrt{a\nu_{bf}}\,xf(\xi)\\&\vartheta(\xi)=\frac{T-T_{in}}{T_w-T_{in}},n(\xi)=\frac{N-N_{in}}{N_{in}},m(\xi)=\frac{M-M_{in}}{M_w-M_{in}}\end{aligned}\right\} \tag{07}$$

The stream capability $\omega$ is characterized as $u_x=\frac{\partial\omega}{\partial y}=axf'(\xi)$ and $u_y=-\frac{\partial\omega}{\partial x}=-\left(a\nu_{bf}\right)^{\frac{1}{2}}f(\xi)$.

The local skin friction coefficient, local Nusselt number, local Sherwood number and local microorganism number are defined as

$$\left.\begin{aligned}&Cf_x=\frac{2\mu_{hnf}}{\rho U^2}\left(\frac{\partial u_x}{\partial y}\right)_{y=0},Nu_x=-\frac{x\kappa_{hnf}}{T_w-T_{in}}\left(\left(\frac{\partial T}{\partial y}\right)_{y=0}+q_r\right)\\&Sh_x=-\frac{xD_{BM}}{C_w-C_{in}}\left(\frac{\partial C}{\partial y}\right)_{y=0}.Nm_x=-\frac{xD_{MO}}{M_w-M_{in}}\left(\frac{\partial M}{\partial y}\right)_{y=0}\end{aligned}\right\} \tag{08}$$

The continuity Eq. in (02) is satisfied for the above-mentioned transformation and the transformed systems of equations are

$$\left.\begin{aligned}&\frac{\mu_{hnf}}{\mu_{bf}}\left(1+\beta^{-1}\right)f'''+\frac{\rho_{hnf}}{\rho_{bf}}\left\{ff''-(f')^2\right\}-\frac{\sigma_{hnf}}{\sigma_{bf}}M_F(f'-\delta)=0\\&\frac{\kappa_{hnf}}{\kappa_{bf}}\frac{1}{Pr}(1+RD)\vartheta''+\frac{\left(\rho c_p\right)_{hnf}}{\left(\rho c_p\right)_{bf}}\left\{f\vartheta'+N_{BM}\vartheta'h'+N_{TP}(\vartheta')^2\right\}=0\\&h''+Le.fh'+\frac{N_{TP}}{N_{BM}}\vartheta''=0\\&m''+Pr.Lb.fm'-Pe\left\{m'h'+(h''+h)(m+\Upsilon)\right\}=0\end{aligned}\right\} \tag{09}$$

The associated boundary conditions are

$$\left.\begin{aligned}&f(0)=0,f'(0)=1,\vartheta(0)=1,N_{BM}\vartheta'(0)+N_{TP}h'(0)=0,m(0)=1\\&f'\to\delta,\vartheta\to0,h\to0,m\to0\ as\ \xi\to\infty\end{aligned}\right\} \tag{10}$$

The dimensionless parameters presented in (09-10) are

$$\left.\begin{aligned}&M_F=\frac{\sigma B_0^2}{2\left(\rho c_p\right)_{bf}U},\delta=\frac{U_{in}}{U_w},RD=\frac{16\sigma^* T_{in}^3}{3k\kappa_{bf}\left(\rho c_p\right)_{bf}},Pr=\frac{\nu_{bf}}{\alpha_{bf}},N_{BM}=\frac{\tau D_{BM}C_{in}}{\nu_{bf}},\\&N_{TP}=\frac{\tau D_{TP}\left(T_w-T_{in}\right)}{T_{in}\nu_{bf}},Le=\frac{\alpha_{bf}}{D_{BM}},Lb=\frac{\alpha_{bf}}{D_{MO}},Pe=\frac{bW_c}{D_{MO}},\Upsilon=\frac{M_{in}}{M_w-M_{in}},\varpi=\frac{U}{U_w}\end{aligned}\right\} \tag{11}$$

Also, the reduced dimensionless physical quantities are

Skin friction $Cfr = \frac{1}{(1-\varphi_1)^{2.5}(1-\varphi_2)^{2.5}} f''(0)$, Nusselt number, $Nur = -\frac{\kappa_{hnf}}{\kappa_{bf}}(1+RD)\vartheta'(0)$, Sherwood number for nanoparticles, $Shr = -n'(0)$, Microorganism's number, $Mor = -m'(0)$

**SOLUTION TECHNIQUES:**

The changed overseeing Conditions (09) alongside the limit conditions (10) are switched over completely to introductory worth issue and are tackled utilizing RKF-45 strategy with the assistance of shooting method

$$\begin{bmatrix} f & \vartheta & n & m \\ f' & \vartheta' & n' & m' \\ f'' & \vartheta'' & n' & m'' \\ f''' & 0 & 0 & 0 \end{bmatrix} = \begin{bmatrix} d_1 & d_4 & d_6 & d_8 \\ d_2 & d_5 & d_7 & d_9 \\ d_3 & d_5' & d_7' & d_9' \\ d_3' & 0 & 0 & 0 \end{bmatrix} \tag{12}$$

Using the above relations, the Equations (09) are converted to first order equations as follows:

$$\begin{pmatrix} d_1' \\ d_2' \\ d_3' \\ d_4' \\ d_5' \\ d_6' \\ d_7' \\ d_8' \\ d_9' \end{pmatrix} = \begin{pmatrix} d_2 \\ d_3 \\ \frac{1}{\frac{\mu_{hnf}}{\mu_{bf}}(1+\beta^{-1})}\left\{\frac{\rho_{hnf}}{\rho_{bf}}\left(d_1 d_3 - d_2^2\right) - \frac{\sigma_{hnf}}{\sigma_{bf}} M_F\left(d_2 - \delta\right)\right\} \\ d_5 \\ -\frac{Pr}{(1+RD)}\frac{\kappa_{bf}}{\kappa_{hnf}}\frac{\left(\rho c_p\right)_{hnf}}{\left(\rho c_p\right)_{bf}}\left\{d_1 d_5 + N_{BM} d_5 d_7 + N_{TP} {d_5}^2\right\} \\ d_7 \\ -\left(Le.d_1 d_7 + \frac{N_{TP}}{N_{BM}} d_5'\right) \\ d_9 \\ -\left[Pr.Lb.d_1 d_9 - Pe\left\{d_7 d_9 + \left(d_8 + \Upsilon\right)\left(d_6 + d_7'\right)\right\}\right] \end{pmatrix} \tag{13}$$

The associated initial conditions are

$$\left.\begin{aligned} &d_1(a) = 0, d_2(a) = 1, d_3(a) = \alpha_1, d_4(a) = 1, d_5(a) = \alpha_2, \\ &d_6(a) = \alpha_3, d_7(a) = -\frac{N_{BM}}{N_{TP}}\alpha_2, d_8(a) = 1, d_9(a) = \alpha_4 \end{aligned}\right\} \tag{14}$$

In the above starting worth issue, five circumstances are known and the excess $(\alpha_1, \alpha_2, \alpha_3, \alpha_4)$ still up in the air by utilizing shooting strategy. Afterward, the calculations are performed by setting $\xi = 10$ for the far field limit conditions and are addressed utilizing RKF-45 request technique with a precision of $10^{-5}$. This technique decides the legitimate step size and at each step, two approximations are made and analyzed. In the event that these two approximations hold close concurrence with one another, it is acknowledged. Else, the step size is additionally diminished and the calculation is rehashed until required exactness is accomplished. The outcome is confirmed by contrasting it and the current writing and the correlation is shown in Table 3.

**Table 3: Validation of results:**

| $Pr$ | $\vartheta'(0)$ | | |
|---|---|---|---|
| | Qasim et al. [39] | Suleman et al. [40] | Present work |
| 0.72 | 1.23664 | 1.23665 | 1.23665 |
| 1 | 1.0000 | 1.0000 | 1.0000 |
| 6.7 | 0.3333 | 0.33331 | 0.33332 |
| 10 | 0.26876 | 0.26877 | 0.26876 |

**STATISTICAL ANALYSIS:**

From table 4, the creators have processed the coefficients of relationship ( $r$ ) between the different relevant components of the stream and actual amounts and introduced them in table 5. Here we can see that all the connection is huge as their qualities are exceptionally near +1 or - 1. Likewise utilizing the information from table 5, creators have assessed the qualities coefficients of assurance ( $D = r^2$ ) in table 6, which empowers us to check up the strength of affiliation and control of fitting variable of the stream on the actual amounts.

**Table 4: Values of physical quantities for various values of flow factors:**

| $N_{BM}$ | $N_{TP}$ | $M_F$ | *Cfr* | | *Nur* | | *Shr* | | *Mor* | |
|---|---|---|---|---|---|---|---|---|---|---|
| | | | Base fluid | Ag-$TiO_2$ Nanofluid | Base fluid | Ag-$TiO_2$ Nanofluid | Base fluid | Ag-$TiO_2$ Nanofluid | Base fluid | Ag-$TiO_2$ Nanofluid |
| 0.1 | | | 1.54201 | 1.48953 | 0.30804 | 0.32454 | 0.43577 | 0.49166 | 0.45129 | 0.51214 |
| 0.3 | | | 1.53894 | 1.47650 | 0.32419 | 0.34522 | 0.45723 | 0.51223 | 0.46512 | 0.52365 |
| 0.5 | 0.2 | 0.5 | 1.51224 | 1.46234 | 0.33298 | 0.35221 | 0.46870 | 0.52873 | 0.47858 | 0.53248 |
| 0.7 | | | 1.50114 | 1.44234 | 0.33851 | 0.36875 | 0.47582 | 0.53854 | 0.48612 | 0.54214 |
| 0.9 | | | 1.49885 | 1.42012 | 0.34229 | 0.38445 | 0.48067 | 0.55231 | 0.49656 | 0.55648 |
| | 0.1 | | 1.53449 | 1.47056 | 0.42152 | 0.44151 | 0.47314 | 0.53454 | 0.49215 | 0.63846 |
| | 0.3 | | 1.54414 | 1.47715 | 0.37920 | 0.39784 | 0.47015 | 0.51223 | 0.47561 | 0.63155 |
| 0.3 | 0.5 | 0.5 | 1.55115 | 1.48120 | 0.34519 | 0.37514 | 0.46707 | 0.50265 | 0.46215 | 0.62526 |
| | 0.7 | | 1.56778 | 1.49024 | 0.31717 | 0.34985 | 0.46398 | 0.49235 | 0.45261 | 0.61949 |
| | 0.9 | | 1.56898 | 1.51021 | 0.29364 | 0.30001 | 0.46091 | 0.47231 | 0.44521 | 0.61414 |
| | | 0.0 | 1.51226 | 1.47225 | 0.32460 | 0.40121 | 0.30124 | 0.42516 | 0.40125 | 0.52164 |
| 0.3 | 0.2 | 0.3 | 1.52331 | 1.48954 | 0.32966 | 0.42151 | 0.32514 | 0.44215 | 0.42151 | 0.54241 |
| | | 0.6 | 1.54199 | 1.49235 | 0.33259 | 0.44556 | 0.33989 | 0.46587 | 0.44265 | 0.56231 |

| | | | | | | | | |
|---|---|---|---|---|---|---|---|---|
| | 0.9 | 1.55112 | 1.50784 | 0.33447 | 0.46554 | 0.36542 | 0.48562 | 0.46521 | 0.58289 |
| | 1.2 | 1.56224 | 1.51264 | 0.33577 | 0.48215 | 0.38945 | 0.50231 | 0.48332 | 0.60314 |

It is seen that Brownian movement has a huge negative effect on skin grinding of the stream, while it has a profoundly certain effect on warmth and mass exchange capacity of the stream. Yet, on the opposite thermophoresis has a positive effect on skin contact however negative impact on warmth and mass exchange of both nanoparticles and microorganisms. It is also witnessed that external magnetic field has elevates the all around performance of the flow system in all factors.

**Table 5: Correlation of Coefficients ( $r$ ) between various factors with various physical quantities:**

| $r$ | *Cfr* | | *Nur* | | *Shr* | | *Mor* | |
|---|---|---|---|---|---|---|---|---|
| | Base fluid | Ag-$TiO_2$ Nanofluid | Base fluid | Ag-$TiO_2$ Nanofluid | Base fluid | Ag-$TiO_2$ Nanofluid | Base fluid | Ag-$TiO_2$ Nanofluid |
| $N_{BM}$ | -0.98343 | -0.95642 | 0.965548 | 0.97457 | 0.96475 | 0.96847 | 0.94227 | 0.94851 |
| $N_{TP}$ | 0.97596 | 0.944587 | -0.96551 | -0.98674 | -0.98594 | -0.98644 | -0.9649 | -0.97388 |
| $M_F$ | 0.99277 | 0.98556 | 0.96784 | 0.97870 | 0.97676 | 0.979221 | 0.96781 | 0.97092 |

**Table 6: Coefficients of Determinations ( $D$ ) between various factors with various physical quantities:**

| $D = r^2$ | *Cfr* | | *Nur* | | *Shr* | | *Mor* | |
|---|---|---|---|---|---|---|---|---|
| | Base fluid | Ag-$TiO_2$ Nanofluid | Base fluid | Ag-$TiO_2$ Nanofluid | Base fluid | Ag-$TiO_2$ Nanofluid | Base fluid | Ag-$TiO_2$ Nanofluid |
| $N_{BM}$ | 0.967135 | 0.914739 | 0.932283 | 0.949787 | 0.930743 | 0.937934 | 0.887873 | 0.899671 |
| $N_{TP}$ | 0.952498 | 0.892245 | 0.93221 | 0.973656 | 0.972078 | 0.973064 | 0.931032 | 0.948442 |
| $M_F$ | 0.985592 | 0.971329 | 0.936714 | 0.957854 | 0.95406 | 0.958874 | 0.936656 | 0.942686 |

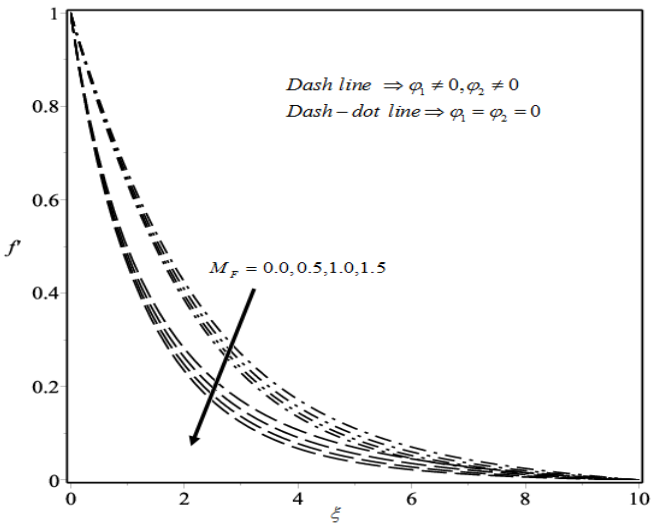


**Figure 2 Velocities under the influence of $M_F$**

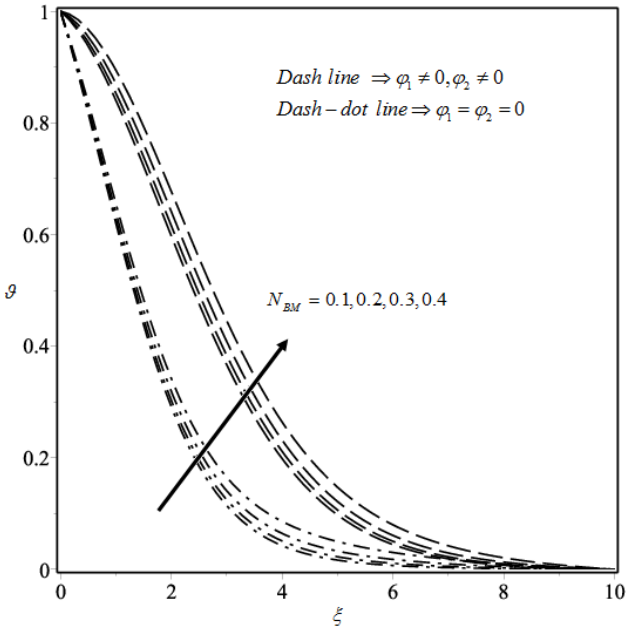


**Figure 3 Temperature under the influence of $N_{BM}$**

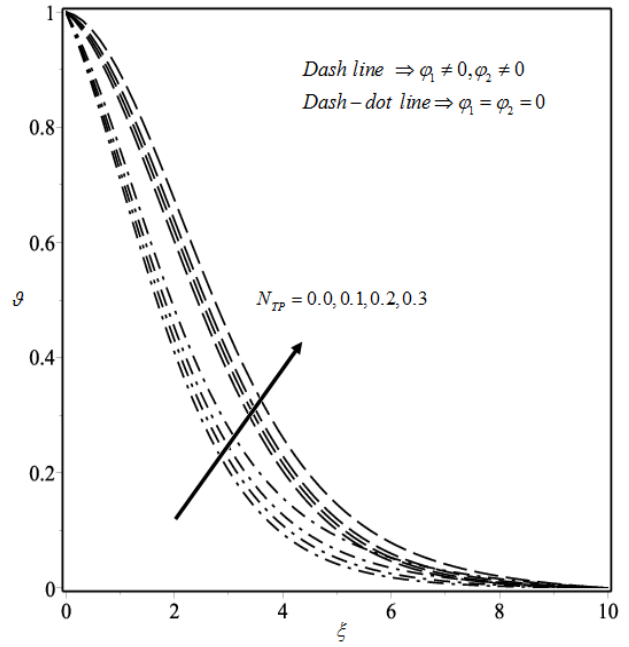


**Figure 4 Temperature under the influence of $N_{TP}$**

**RESULT AND DISCUSSIONS:**

The mathematical calculations have been performed to investigate the impact of different boundaries on the temperature, focus and microorganism's thickness profile. The outcomes are acquired as diagrams outlines including the way of behaving of skin grinding coefficient, Nusselt number, and motile thickness number. We are centered on the examination of the outcomes between base fluid and $Ag+TiO_2/H_2O$ hybrid nanofluid.

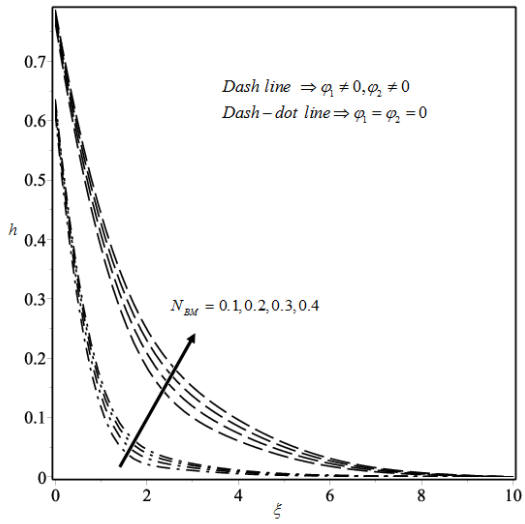


**Figure 5 Fluid densities under the influence of $N_{BM}$**

We observe in figure 2 that the velocity of the flow is constantly diminishes with higher magnitude of external magnetic field as this elevates the Lorentz force that increases the drag force in the flow. But in nanofluid flow it is highly effective to hinder the flow due to the presence of metallic nanoparticles.

Also, we are interested to overview the effects of Brownian motion and thermophoresis in the flow character. In figure 3, it is staged that temperature of the flow risen up with higher Brownian motion in the particles. And obviously it is better effective in the flow with nanoparticles in it. Similarly, thermophoretic event also elevates the temperature of the flow and more significantly in hybrid nanofluid flow as shown in figure 4.

The influences of Brownian motion and thermophoresis on the nanoparticle density are staged in figures 5-6. Here we've seen that density is increased with higher Brownian motion and thermophoresis event. Also flow concentration is much higher in hybrid nanofluid flow.

It is interesting to observe that the presence of nanoparticles in the flow mark the effects of Brownian motion and thermophoresis on the micro-organism density of the flow in figures 7-8. Both $N_{BM}$ and $N_{TP}$ increase the micro-organism density of the flow.

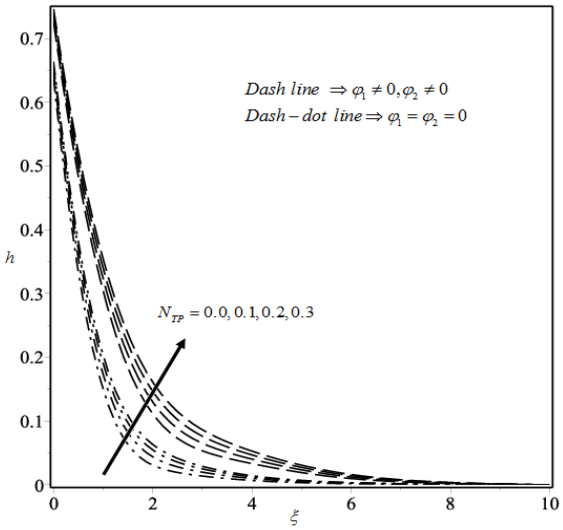


**Figure 6 Fluid densities under the influence of $N_{TP}$**

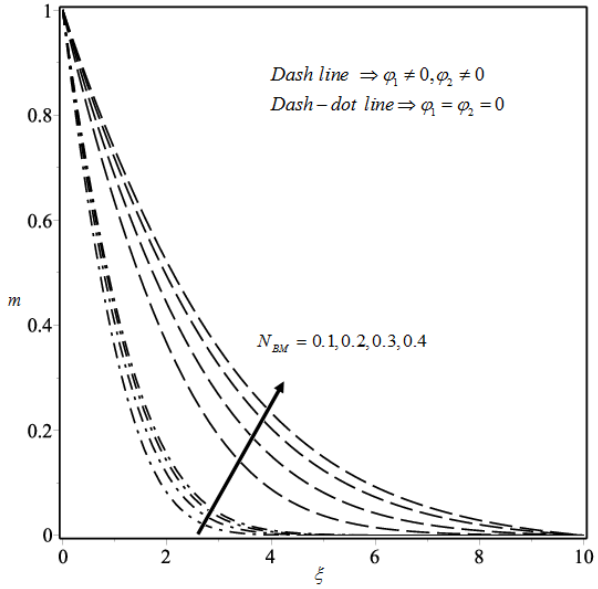


**Figure 7 Microorganism densities under the influence of $N_{BM}$**

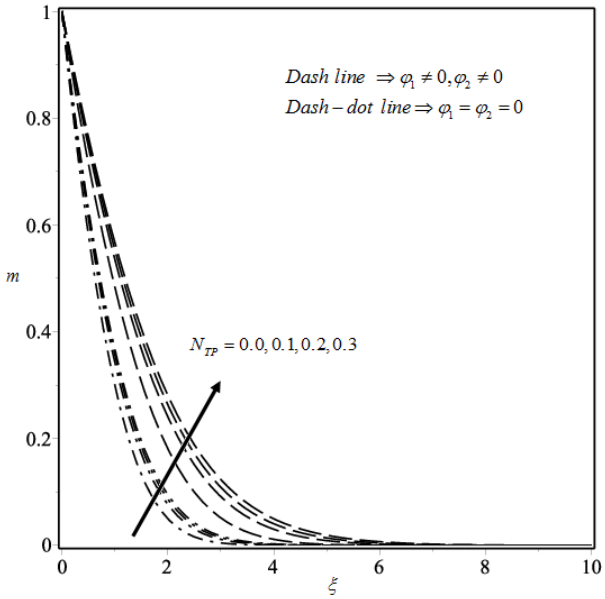


**Figure 7 Microorganism densities under the influence of $N_{TP}$**

**CONCLUDING REMARKS:**

After cautiously noticing the bioconvective Casson stream of hybrid nanofluid with gyrotactic microorganisms over vertical slendering plate, we came to the accompanying perceptions.

- Externally applied magnetic force increase the overall performance of the flow like in heat transmission and mass transmission.
- Brownian motion and thermophoresis both have significant influence in characteristics of the flow. And more influence in hybrid nanofluid flow.
- Due to the presence of metallic nanoparticles in the base fluid, Brownian motion and thermophoresis are able to regulate the temperature, density etc. of the flow more prominently.
- We can regulate the performance of the flow by regulating the magnetic field, Brownian motion, thermophoresis to obtain the highest level of efficiency of the system.

**REFERANCES**

[1] Platt, J. R., 1961, "'Bioconvection Patterns' in Cultures of Free-Swimming Organisms," Science, 133(3466), pp. 1766–1767.
[2] Ghorai, S., and Hill, N., 2000, "Wavelengths of Gyrotactic Plumes in Bio- convection," Bull. Math. Biol., 62(3), pp. 429–450.
[3] Choi, S. U., and Eastman, J. A., 1995, "Enhancing Thermal Conductivity of Fluids with Nanoparticles," Argonne National Lab, Lemont, IL, Report No. ANL/MSD/CP-84938.
[4] Xuan, Y., and Roetzel, W., 2000, "Conceptions for Heat Transfer Correlation of Nanofluids," Int. J. Heat Mass Transfer, 43(19), pp. 3701–3707.
[5] Xuan, Y., and Li, Q., 2000, "Heat Transfer Enhancement of Nanofluids," Int. J. Heat Fluid Flow, 21(1), pp. 58–64.
[6] Sinha, A., and Misra, J., 2014, "Effect of Induced Magnetic Field on Magneto- hydrodynamic Stagnation Point Flow and Heat Transfer on a Stretching Sheet," ASME J. Heat Transfer, 136(11), p. 112701.
[7] Basir, M. F. M., Uddin, M., and Ismail, A., 2017, "Unsteady Magnetoconvec- tive Flow of Bionanofluid With Zero Mass Flux Boundary Condition," Sains Malays., 46(2), pp. 327–333.
[8] Reddy, N. B., Poornima, T., and Sreenivasulu, P., 2016, "Radiative Heat Trans- fer Effect on MHD Slip Flow of Dissipating Nanofluid Past an Exponential Stretching Porous Sheet," Int. J. Pure Appl. Math., 109(9), pp. 134–142.
[9] Sreenivasulu, P. ., Poornima, T. ., and Bhaskar Reddy, N. ., 2016, "Thermal Radiation Effects on MHD Boundary Layer Slip Flow past a Permeable Expo- nential Stretching Sheet in the Presence of Joule Heating and Viscous Dis- sipation," J. Appl. Fluid Mech., 9(1), pp. 267–278.
[10] Parida, S., Panda, S., and Rout, B., 2015, "MHD Boundary Layer Slip Flow and Radiative Nonlinear Heat Transfer Over a Flat Plate with Variable Fluid Prop- erties and Thermophoresis," Alexandria Eng. J., 54(4), pp. 941–953.
[11] Nayak, M., Shaw, S., and Chamkha, A. J., 2018, "Impact of Variable Magnetic Field and Convective Boundary Condition on a Stretched 3D Radiative Flow of Cu-$H_2O$ Nanofluid," AMSE JOURNALS-AMSE IIETA Series: Modelling B, 86(3), pp. 658–678.
[12] Nayak, M., Akbar, N., Tripathi, D., and Pandey, V., 2017, "Three Dimensional MHD Flow of Nanofluid Over an Exponential Porous Stretching Sheet with Convective Boundary Conditions," Therm. Sci. Eng. Prog., 3, pp. 133–140.
[13] Das, S., Sensharma, A., Jana, R., and Sharma, R., 2017, "Slip Flow of Nano- fluid Past a Vertical Plate with Ramped Wall Temperature Considering Ther- mal Radiation," J. Nanofluids, 6(6), pp. 1054–1064.
[14] Kuznetsov, A., 2005, "The Onset of Bioconvection in a Suspension of Gyrotac- tic Microorganisms in a Fluid Layer of Finite Depth Heated From Below," Int. Commun. Heat Mass Transfer, 32(5), pp. 574–582.
[15] Kuznetsov, A., 2005, "Thermo-Bioconvection in a Suspension of Oxytactic Bacteria," Int. Commun. Heat Mass Transfer, 32(8), pp. 991–999.
[16] Kuznetsov, A., 2005, "Investigation of the Onset of Thermo-Bioconvection in a Suspension of Oxytactic Microorganisms in a Shallow Fluid Layer Heated from Below," Theor. Comput. Fluid Dyn., 19(4), pp. 287–299.
[17] Kuznetsov, A., 2006, "The Onset of Thermo-Bioconvection in a Shallow Fluid Saturated Porous Layer Heated from Below in a Suspension of Oxytactic Microorganisms," Eur. J. Mech.-B, 25(2), pp. 223–233.
[18] Aziz, A., Khan, W., and Pop, I., 2012, "Free Convection Boundary Layer Flow Past a Horizontal Flat Plate Embedded in Porous Medium Filled by Nanofluid Containing Gyrotactic Microorganisms," Int. J. Therm. Sci., 56, pp. 48–57.
[19] Tham, L., Nazar, R., and Pop, I., 2013, "Mixed Convection Flow Over a Solid Sphere Embedded in a Porous Medium Filled by a Nanofluid Containing Gyro- tactic Microorganisms," Int. J. Heat Mass Transfer, 62, pp. 647–660.
[20] Tham, L., Nazar, R., and Pop, I., 2013, "Steady Mixed Convection Flow on a Horizontal

Circular Cylinder Embedded in a Porous Medium Filled by a Nano- fluid Containing Gyrotactic Micro-Organisms," ASME J. Heat Transfer, 135(10), p. 102601.
[21] Shaw, S., Kameswaran, P., Narayana, M., and Sibanda, P., 2014, "Bioconvection in a Non-Darcy Porous Medium Saturated with a Nanofluid and Oxytactic Micro-Organisms," Int. J. BioMath., 7(1), p. 1450005.
[22] Balla, C. S., Haritha, C.., Naikoti, K., and Rashad, A. M., 2019, "Bioconvection in Nanofluid-Saturated Porous Square Cavity Containing Oxy- tactic Microorganisms," Int. J. Numer. Methods Heat and Fluid Flow, 29(4), pp. 1448–1465.
[23] Sheremet, M. A., and Pop, I., 2014, "Thermo-Bioconvection in a Square Porous Cavity Filled by Oxytactic Microorganisms," Transp. Porous Media, 103(2), pp. 191–205.
[24] Khan, W., and Makinde, O., 2014, "MHD Nanofluid Bioconvection Due to Gyrotactic Microorganisms Over a Convectively Heat Stretching Sheet," Int. J. Therm. Sci., 81, pp. 118–124.
[25] Khan, W., Makinde, O., and Khan, Z., 2014, "MHD Boundary Layer Flow of a Nanofluid Containing Gyrotactic Microorganisms Past a Vertical Plate With Navier Slip," Int. J. Heat Mass Transfer, 74, pp. 285–291.
[26] Gireesha, B., Kumar, K. G., and Manjunatha, S., 2018, "Impact of Chemical Reaction on MHD 3D Flow of a Nanofluid Containing Gyrotactic Microorgan- ism in the Presence of Uniform Heat Source/Sink," Int. J. Chem. React. Eng., 16(12), p. 20180013.
[27] Gireesha, B. J., Kumar, K. G., Rudraswamy, N., and Manjunatha, S., 2018, "Effect of Viscous Dissipation on Three Dimensional Flow of a Nanofluid by Considering a Gyrotactic Microorganism in the Presence of Convective Con- dition," Defect Diffus. Forum, 388, pp. 114–123.
[28] Hayat, T., and Nadeem, S., 2017, "Heat Transfer Enhancement with Ag–CuO/ Water Hybrid Nanofluid," Results Phys., 7, pp. 2317–2324.
[29] Tayebi, T., and Chamkha, A. J., 2020, "Entropy Generation Analysis Due to MHD Natural Convection Flow in a Cavity Occupied with Hybrid Nanofluid and Equipped With a Conducting Hollow Cylinder," J. Therm. Anal Calorim., 139(3), pp. 2165–2179.
[30] Ghalambaz, M., Doostani, A., Izadpanahi, E., and Chamkha, A. J., 2020, "Conjugate Natural Convection Flow of Ag–MgO/Water Hybrid Nanofluid in a Square Cavity," J. Therm. Anal. Calorim., 139(3), pp. 2321–2336.
[31] Dogonchi, A., Nayak, M., Karimi, N., Chamkha, A. J., and Ganji, D. D., 2020, "Numerical Simulation of Hydrothermal Features of Cu–$H_2O$ Nanofluid Natural Convection Within a Porous Annulus Considering Diverse Configura- tions of Heater," J. Therm. Anal Calorim., 141, pp. 2109–2125.
[32] Manjunatha, S., Kuttan, B. A., Jayanthi, S., Chamkha, A., and Gireesha, B., 2019, "Heat Transfer Enhancement in the Boundary Layer Flow of Hybrid Nanofluids Due to Variable Viscosity and Natural Convection," Heliyon, 5(4), p. e01469.
[33] Sung-Suh, H. M., Choi, J. R., Hah, H. J., Koo, S. M., and Bae, Y. C., 2004, "Comparison of ag Deposition Effects on the Photocatalytic Activity of Nano- particulate $TiO_2$ Under Visible and UV Light Irradiation," J. Photochem. Photo- Biol. A, 163(1–2), pp. 37–44.
[34] Sclafani, A., and Herrmann, J.-M., 1998, "Influence of Metallic Silver and of Platinum-Silver Bimetallic Deposits on the Photocatalytic Activity of Titania (Anatase and Rutile) in Organic and Aqueous Media," J. Photochem. Photo- Biol. A, 113(2), pp. 181–188.
[35] Yin, S., Hasegawa, H., Maeda, D., Ishitsuka, M., and Sato, T., 2004, "Synthesis of Visible-Light-Active Nanosize Rutile Titania Photocatalyst by Low Temper- ature Dissolution–Reprecipitation Process," J. Photochem. PhotoBiol. A, 163(1–2), pp. 1–8.
[36] Amirsom, N., Uddin, M. J., and Ismail, A. I. M., 2019, "MHD Boundary Layer Bionanoconvective Non-Newtonian Flow Past a Needle with Stefan Blowing," Heat Transfer, 48(2), pp. 727–743.
[37] Rosseland, S., 2013, Astrophysik: Auf Atomtheoretischer Grundlage, Vol. 11, Springer-Verlag, Berlin.
[38] Tian, X.-Y., Li, B.-W., and Zhang, J.-K., 2017, "The Effects of Radiation Optical Properties on the Unsteady 2D Boundary Layer MHD Flow and Heat Transfer Over a Stretching Plate,"

Int. J. Heat Mass Transfer, 105, pp. 109–123.

[39] Qasim, M., Khan, Z. H., Khan, W. A., and Shah, I. A., 2014, "MHD Boundary Layer Slip Flow and Heat Transfer of Ferrofluid Along a Stretching Cylinder with Prescribed Heat Flux," PLoS One, 9(1), p. e83930.

[40] Suleman, M., Ramzan, M., Ahmad, S., Lu, D., Muhammad, T., and Chung, J. D., 2019, "A Numerical Simulation of Silver–Water Nanofluid Flow with Impacts of Newtonian Heating and Homogeneous–Heterogeneous Reactions Past a Nonlinear Stretched Cylinder," Symmetry, 11(2), p. 295.